HOKKAIDO UNIVERSITY

Title	Generalization of microscopic multipoles and cross-correlated phenomena by their orderings
Author(s)	Kusunose, Hiroaki; Hayami, Satoru
Citation	Journal of physics : condensed matter, 34(46), 464002 https://doi.org/10.1088/1361-648X/ac9209
Issue Date	2022-11-16
Doc URL	http://hdl.handle.net/2115/90709
Rights	This is the Accepted Manuscript version of an article accepted for publication in Journal of Physics : Condensed Matter. IOP Publishing Ltd is not responsible for any errors or omissions in this version of the manuscript or any version derived from it. The Version of Record is available online at https://doi.org/10.1088/1361-648X/ac9209.
Rights(URL)	https://creativecommons.org/licenses/by-nc-nd/4.0/
Type	article (author version)
File Information	J. Phys.-Condes. Matter_34(46)_464002.pdf

Instructions for use

Hokkaido University Collection of Scholarly and Academic Papers : HUSCAP

Generalization of microscopic multipoles and cross-correlated phenomena by their orderings

Hiroaki Kusunose[1] **& Satoru Hayami**[2]

[1]Department of Physics, Meiji University, Kawasaki 214-8571, Japan
[2]Department of Applied Physics, the University of Tokyo, Tokyo 113-8656, Japan

E-mail: hk@meiji.ac.jp

Abstract. The generalization of the atomic-scale multipoles is discussed. By introducing the augmented multipoles defined in the hybrid orbitals or in the site/bond-cluster, any of electronic degrees of freedom can be expressed in accordance with the crystallographic point group. These multipoles are useful to describe the cross-correlated phenomena, band-structure deformation, and generation of effective spin-orbit coupling due to antiferromagnetic ordering in a systematic and comprehensive manner. Such a symmetry-adapted multipole basis set could be a promising descriptor for materials design and informatics.

1. Introduction

Diversity of physical phenomena is the most attractive feature in condensed matter physics. Although an electron has only charge and spin degrees of freedom in a vacuum, it acquires many nontrivial degrees of freedom in crystals, exhibiting a wide variety of physical responses through their mutual interplay. It is to say that the most of research on electronic properties in solids is the search for nontrivial degrees of freedom, their realization in specific materials, and clarification of quirky physical properties brought about by such degrees of freedom. Nevertheless, diversity often tends to lead to merely complexity such as a specific physical property in a specific material, giving an impression of the absence of universality.

Symmetry is a suitable concept that unifies systematically the various degrees of freedom of electrons in crystals. For example, macroscopic physical responses to external fields, such as electrical conductivity, elastic constants and so on, are determined completely by the macroscopic symmetry of a system. The symmetry of an electronic system is not only determined by that of its crystal structure, but also by the spontaneous symmetry breaking due to the emergence of long-range order, and its physical properties change accordingly. In the Landau's phenomenological theory of phase transitions, physical properties are discussed by considering candidate order parameters, whose interactions are taken into account by introducing a free energy that satisfies the full symmetry of a disordered phase. It is a natural approach to examining the physical properties of crystals in a universal manner since the symmetry is closely related to their emergence, and have succeeded especially in describing peculiar phases in rare-earth and actinide compounds, which contain a large number of orbitals that are entangled with spins by strong spin-orbit coupling.

In the early stage of research, atomic-scale multipoles have been introduced to describe systematically such entangled degrees of freedoms in f-electron systems. The exotic features of

type	symbol	spatial inversion	time reversal	monopole	dipole	quadrupole	octupole
E	Q_{lm}	$(-1)^l$ polar	$+$	$(+,+)$	E ET		
M	M_{lm}	$(-1)^{l+1}$ axial	$-$	$(-,-)$	M MT		
MT	T_{lm}	$(-1)^l$ polar	$-$	$(+,-)$	MT M		
ET	G_{lm}	$(-1)^{l+1}$ axial	$+$	$(-,+)$	ET E		

Figure 1. Four types of multipoles and their parities with respect to space-time reversals [8]. They are abbreviated as electric multipole (E), magnetic multipole (M), magnetic toroidal multipole (MT), and electric toroidal multipole (ET), respectively, and denoted by the symbols, Q, M, T, and G.

hidden orders and their multiferroic responses have been unveiled by using higher-rank atomic-scale multipoles [1, 2, 3, 4]. However, under the restriction to the Hilbert space within one type of orbital in a single atom, there exist transitions only between the states with the same spatial parity, so that the even-parity electric and magnetic multipoles only become active. In recent years, a generalization of microscopic multipoles has been carried out in the direction to include other degrees of freedoms to describe such as the odd-parity systems, by expanding the Hilbert space to plural types of orbitals in a cluster of atoms in a unit cell in accordance with their symmetries [5, 6, 7, 8, 9, 10, 11].

In this paper, we first introduce four types of augmented microscopic multipoles with definite spatial and time-reversal parities, which can be used as the complete basis set to describe any electronic degrees of freedom. In the following sections, the classification of augmented multipoles and cross-correlated phenomena by them, and the outline of some examples of their applications are given [7, 8, 12, 13, 14, 15, 16, 17].

2. Four types of multipoles

The concept of multipoles appears in classical electromagnetism as a quantity to characterize the anisotropy of the source charge and electric current distributions of an electromagnetic field [18, 19, 20]. In this context, the electric and magnetic multipoles are well known. A quantity with the same spatial parity as a polynomial of position vector $\boldsymbol{r}$, i.e, $(-1)^l$ is called "polar", and one with the opposite parity $(-1)^{l+1}$ is "axial", where l is the rank of a multipole. In addition, the electric charge (current) is even (odd) parity in terms of the time-reversal operation. Thus, the electric (magnetic) multipole is characterized by a polar (an axial) tensor with time-reversal even (odd). There also exist less familiar multipoles, i.e., toroidal multipoles, which have opposite spatial parities with conventional electric and magnetic multipoles [21, 22, 23, 24, 25, 26, 27, 28]. The conventional and toroidal multipoles are related with each other by the contraction procedure with $\boldsymbol{r}\times$ or $\sum_{jk}\epsilon_{ijk}r_jX_{k\cdots}$ (ϵ_{ijk} is the Levi-Civita

fully anti-symmetric tensor). For example, a quantity consisting of the vortex-like arrangement of the electric dipoles is characterized by an electric toroidal dipole, while that of magnetic dipoles by a magnetic toroidal dipole, and so on. These four types of multipoles with their space-time parities are shown in Fig. 1. Note that the even-rank polar and odd-rank axial multipoles are even parity, while the odd-rank polar and even-rank axial multipoles are odd parity.

The three types of multipoles except for the electric toroidal multipoles have long been known because they appear in multipole expansions of scalar and vector potentials. On the other hand, the electric toroidal multipole was introduced around the mid 1980s as a useful quantity to describe macroscopic electric axial quantities [22]. In order to describe these multipoles quantum mechanically, operator expressions corresponding to these classical multipoles are necessary. They can be directly derived from their classical definitions for three types of multipoles [1]. However, since the electric toroidal multipole does not appear in the multipole expansions, its operator expression was obtained only quite recently [7, 11]. Once the operator expressions of these four types of multipoles are obtained, one can construct a complete basis set in terms of these operators to describe any electronic degrees of freedom. In other words, arbitrary electronic degrees of freedom, not only in the restricted atomic states in one type of orbital in a single atom, but also in any Hilbert space of plural types of orbitals in a cluster of atoms in a unit cell can be expressed by a complete basis set of multipoles, as shown in the following sections.

Multipoles are usually classified according to the parities with respect to space-time inversions, and the irreducible representations of the rotation group, i.e., the orbital angular momentum and its component, l and m. Since the crystallographic point group is a subgroup of the rotation group, its irreducible representation is represented by a linear combination of those of the rotation group. Therefore, the four types of multipole operators can be used to represent any electronic degrees of freedom in crystals as well. In this sense, it is the best representation for classifying any electronic degrees of freedom in accordance with the crystallographic symmetry. The order parameter in the Landau theory is a classical macroscopic quantity to describe the change of the symmetry, while the present multipole operators are regarded as microscopic quantum variables and their expectation values correspond to the order parameters.

According to the Neumann's principle, "The symmetry group of any physical properties of crystals will include the symmetry elements of the point group of the crystal.", the microscopic multipoles classified by the crystallographic point group are sufficient to describe physical response tensors in terms of their expectation values. Although it is often misunderstood that the microscopic multipole description does not contain more than symmetry argument, the presence or absence of microscopic multipoles is closely related to the Hilbert space to consider them, and hence, it depends strongly on the electronic states in question. This point is important to answer why materials with the same crystal structure (symmetry) do not all exhibit the same physical properties. In other words, different electronic states under the same symmetry can exhibit different physical properties, and the difference is reflected in which type of multipole is active or not. It is quite useful to narrow down possible physical responses to occur depending on the active multipoles.

3. Active multipoles, Hilbert space, and order parameters

As mentioned above, the properties of the electronic states are reflected in the active multipoles which determine physical responses. Let us first consider active multipoles for the spinless orbital states within a single atom.

The matrix element $\langle L_1, M_1 | X_{lm} | L_2, M_2 \rangle$ of the multipole operator X_{lm} $(X = Q, M, T, G)$ with respect to the states, $|L, M\rangle$ of the orbital angular momentum L and its component M is proportional to the overlap integral of the spherical harmonics, $\int d\hat{\boldsymbol{r}} Y^*_{L_1 M_1}(\hat{\boldsymbol{r}}) Y_{lm}(\hat{\boldsymbol{r}}) Y_{L_2 M_2}(\hat{\boldsymbol{r}})$. Thus, whether it is active or not is determined by the addition rule of the angular momentum.

Table 1. Active multipoles in the orbital basis, (L_1, L_2)[7]. The number of independent multipoles is indicated in the parenthesis. Even-parity (odd-parity) multipoles are above (below) the middle solid line.

basis		$l=0$	$l=1$	$l=2$	$l=3$	$l=4$	$l=5$	$l=6$
s-*s*	(1)	E	–	–	–	–	–	–
p-*p*	(9)	E	M	E	–	–	–	–
d-*d*	(25)	E	M	E	M	E	–	–
f-*f*	(49)	E	M	E	M	E	M	E
s-*d*	(10)	–	–	E/MT	–	–	–	–
p-*f*	(42)	–	–	E/MT	M/ET	E/MT	–	–
s-*p*	(6)	–	E/MT	–	–	–	–	–
s-*f*	(14)	–	–	–	E/MT	–	–	–
p-*d*	(30)	–	E/MT	M/ET	E/MT	–	–	–
d-*f*	(70)	–	E/MT	M/ET	E/MT	M/ET	E/MT	–

Namely, the multipoles with the rank l satisfying $|L_1 - L_2| \leq l \leq L_1 + L_2$ can be active. Moreover, since the spatial parity of Y_{LM} is $(-1)^L$, it is active only when $(-1)^{L_1+L_2} = (-1)^L$. For instance, when we consider one type of orbital, i.e., $L_1 = L_2$, even-parity multipoles X_{lm} are only active. On the other hand, when $L_1 \neq L_2$, a pair of (E,MT) or (M,ET) with the same spatial parity are active. The active multipoles in different types of orbitals are referred to as "hybrid" multipole. The above selection rules are summarized in Table 1 [7].

A similar discussion can be made for spinful states, $|J, M\rangle$ of the total angular momentum J and its component M. In this case, the selection rule with respect to L becomes slightly complicated since there are two types of orbitals $L = J \pm 1/2$ for half-integer J. The resultant selection rules are summarized in Ref. [8] for example. Note that the explicit expressions of matrix elements for four types of multipoles in the complete basis set are given in Ref. [11].

The number of independent multipole operators is $2(2J_1 + 1)(2J_2 + 1)$ which coincides with the total number of matrix elements in the Hilbert spaces of J_1 and J_2 ($J_1 \neq J_2$), where the pre-factor 2 appears as the off-diagonal matrix elements can be complex[1]. When the symmetry becomes lower from the rotation group to the crystallographic point group, the degeneracy of $|J, M\rangle$ is lifted, and the relevant Hilbert space is narrowed. As a result, some of multipoles that were independent in the rotation group become linearly dependent with each other in the narrowed subspace. This is related to the fact that spherical harmonics (nodal positions) that could be distinguished by the continuous spherical coordinate in the rotation group become indistinguishable in the discrete coordinate in the point group.

Examples of compatibility relation among the irreducible representations in the symmetry lowering[2] is shown in Table 2. It should be emphasized that the multipoles belonging only to the identity irreducible representation can have finite expectation value (A_{1g} , A_1, A_g, A in Table 2 for example). Therefore, a multipole that falls into the identity irreducible representation as a result of symmetry lowering is a candidate of the order parameter of its phase transition.

[1] The number of independent multipoles is $(2J_1 + 1)^2$ for $J_1 = J_2$.

[2] The more detailed table is given in Ref. [8] for example.

Table 2. Compatibility relation of the multipoles (up to rank 2) with the irreducible representation among cubic and tetragonal groups [8]. The even-parity (odd-parity) multipoles are shown in the upper (lower) panel. The subscript, 0, represents monopole, x, y, z are the component of dipole, $u = 3z^2 - r^2$, $v = x^2 - y^2$, yz, zx, xy are the component of quadrupole.

multipole	$O_{\rm h}$	O	$T_{\rm d}$	$T_{\rm h}$	T	$D_{4\rm h}$	D_4	$C_{4\rm h}$	$D_{2\rm d}$	$C_{4\rm v}$	C_4	S_4
Q_0, T_0	A_{1g}	A_1	A_1	A_g	A	A_{1g}	A_1	A_g	A_1	A_1	A	A
—	A_{2g}	A_2	A_2	A_g	A	B_{1g}	B_1	B_g	B_1	B_1	B	B
Q_u, T_u	E_g	E	E	E_g	E	A_{1g}	A_1	A_g	A_1	A_1	A	A
Q_v, T_v						B_{1g}	B_1	B_g	B_1	B_1	B	B
G_x, M_x	T_{1g}	T_1	T_1	T_g	T	E_g	E	E_g	E	E	E	E
G_y, M_y												
G_z, M_z						A_{2g}	A_2	A_g	A_2	A_2	A	A
Q_{yz}, T_{yz}	T_{2g}	T_2	T_2	T_g	T	E_g	E	E_g	E	E	E	E
Q_{zx}, T_{zx}												
Q_{xy}, T_{xy}						B_{2g}	B_2	B_g	B_2	B_2	B	B
G_0, M_0	A_{1u}	A_1	A_2	A_u	A	A_{1u}	A_1	A_u	B_1	A_2	A	B
—	A_{2u}	A_2	A_1	A_u	A	B_{1u}	B_1	B_u	A_1	B_2	B	A
G_u, M_u	E_u	E	E	E_u	E	A_{1u}	A_1	A_u	B_1	A_2	A	B
G_v, M_v						B_{1u}	B_1	B_u	A_1	B_2	B	A
Q_x, T_x	T_{1u}	T_1	T_2	T_u	T	E_u	E	E_u	E	E	E	E
Q_y, T_y												
Q_z, T_z						A_{2u}	A_2	A_u	B_2	A_1	A	B
G_{yz}, M_{yz}	T_{2u}	T_2	T_1	T_u	T	E_u	E	E_u	E	E	E	E
G_{zx}, M_{zx}												
G_{xy}, M_{xy}						B_{2u}	B_2	B_u	A_2	B_1	B	A

4. Cross-correlated response in terms of multipole

The four types of multipoles are closely related to the component of the response tensors [8]. In particular, they are suitable for describing the cross-correlated responses such as the linear magnetoelectric effect, in which magnetization (electric polarization) is induced by an electric field (magnetic field), piezoelectric effect (electric polarization is induced by stress), spin Hall effect, and (thermal) current-induced magnetization. Let us demonstrate the relation by taking the magnetoelectric effect as a typical example. The linear magnetoelectric effect is characterized by the tensor α_{ij}, by which $M_i = \sum_j \alpha_{ij} E_j$ $(i, j = x, y, z)$. α_{ij} has 9 independent components by the combination of 3 input and 3 output. Since the linear relation must be invariant by the rotation of the coordinate axes, α_{ij} transforms like a rank-2 tensor. As the electric field is a polar vector and the magnetic field is an axial vector, the ranks of the multipoles involved in the response tensor are determined as 0, 1, and 2 from the addition law of two vectors (their angular momenta are 1). Thus, the response tensor can be expressed by using scalar X_0, vector $\boldsymbol{X'}$ and second-rank tensor X''_{ij} as $\alpha_{ij} = \delta_{ij} X_0 + \sum_k \epsilon_{ijk} X'_k + X''_{ij}$. The total number of these components, $1 + 3 + 5 = 9$, is the same as that of α_{ij}. α_{ij} is magnetic (odd under time-reversal operation) since electric and magnetic fields have different time-reversal properties. Moreover, α_{ij} connecting polar and axial quantities must be axial. Noting that δ_{ij} and ϵ_{ijk} are the polar and axial tensors, X_0 and X''_{ij} are axial tensors, while $\boldsymbol{X'}$ is polar. Thus, X_0 and X''_{ij} are magnetic

monopole and quadrupole, while $\boldsymbol{X}'$ is magnetic toroidal dipole. It is explicitly expressed as[3]

$$\alpha = \begin{pmatrix} M_0 - M_u + M_v & M_{xy} + T_z & M_{xz} - T_y \\ M_{xy} - T_z & M_0 - M_u - M_v & M_{yz} + T_x \\ M_{xz} + T_y & M_{yz} - T_x & M_0 + 2M_u \end{pmatrix}. \quad (1)$$

The magnetic monopole M_0 describes the isotropic longitudinal response, while the magnetic quadrupole M_{ij} represents the anisotropic symmetric response. On the other hand, the magnetic toroidal dipole T_k is the anti-symmetric component. Both the time-reversal and spatial inversion symmetries must be broken to obtain the finite expectation value of the multipoles appeared in Eq. (1). Moreover, the multipoles belonging to the identity irreducible representation can have finite expectation value. For example, in the point group D_4, M_0 and M_u belong to A_1 from Table 2. Thus, α_{ij} only has diagonal components and $\alpha_{xx} = \alpha_{yy} \neq \alpha_{zz}$ if M_u is finite.

In a similar way, we consider the current-induced magnetization, so-called Edelstein effect. Since the input is replaced as $\boldsymbol{E} \to \boldsymbol{j}$ (from electric to magnetic quantity), the response tensor, $\alpha_{ij}^{\rm CM}$ is the electric axial tensor, and hence the components of Eq. 1 are replaced as $M \to G$ and $T \to Q$ from the symmetry point of view. In this case, only the spatial inversion symmetry breaking is necessary. For example, the elemental Te belonging to the space group of D_3^4 or D_3^6 (the associated point group is D_3) indeed shows the Edelstein effect [29, 30]. Since G_0 and G_u are the identity irreducible representation, only the diagonal components can be finite as $\alpha_{xx}^{\rm CM} = \alpha_{yy}^{\rm CM} \neq \alpha_{zz}^{\rm CM}$. The symmetry argument cannot allow further discussion, however, taking account of the fact that the electronic states near the Fermi energy consist of $J_z = \pm 3/2$, we would obtain $G_0 \sim G_u$. As a result, $\alpha_{xx}^{\rm CM} = \alpha_{yy}^{\rm CM} \sim 0$ [29]. In this way, the multipole description contains the information of the relevant electronic states more than the symmetry.

Although the magnetoelectric and Edelstein effects are characterized by different response tensors, they are both discussed by the current-magnetization response function in the linear-response theory. The difference between them comes from qualitatively different contributions in the response function [31, 8, 16]. Namely, one is the intra-band contribution and the other is the inter-band contribution. The latter is driven essentially by an electric field, which is relevant to the magnetoelectric effect both in metal and insulator, while the former is driven by an electric current that sensitively depends on the purity of a sample. When considering the response to the electric field, discrimination of these contributions is important. Typical cross-correlated responses and the relevant multipoles are summarized in Table 3.

5. Site-cluster multipole

In the previous sections, it has been shown that extending the Hilbert space to plural orbitals makes all four types of multipoles active, and they contribute to response tensors in various cross-correlated phenomena. At present, a representative case involving hybrid multipole has not been found, and further elaborate study would be required on this topic. The actinide compounds and $5d$ systems with strong orbital hybridization, exciton insulators, organic conductors, and quantum dots would be good candidates to explore hybrid multipoles [32, 33, 34, 35, 36, 37, 38].

On the other hand, studies of "cluster" multipoles, which are activated on the multi-site or multi-bond cluster, have been performed extensively in recent years [39, 40, 41, 42, 43, 44, 45, 5, 46, 31, 47, 48, 49, 50, 51, 52, 54, 53, 55]. From the symmetry point of view, complex magnetic structures, such as spiral magnetic order, had better to be treated not in pieces but with a clump by bundling them. This is because the symmetry of the clump, rather than the individual magnetic moment, determines the symmetry of the system, which motivates the introduction of the site-cluster or bond-cluster multipoles. Figure 2(a) shows examples of the site-cluster multipoles. The bond-cluster multipoles are discussed in the next section.

[3] We define $M_0 = (M_{xx} + M_{yy} + M_{zz})/3$, $M_u = (2M_{zz} - M_{xx} - M_{yy})/6$, $M_v = (M_{xx} - M_{yy})/2$

Table 3. Representative cross-correlated responses [8]. $\boldsymbol{E}$, $\boldsymbol{H}$, $-\boldsymbol{\nabla}T$, ε_{ij} represent an electric field, magnetic field, thermal gradient, and strain, respectively. Q, $\boldsymbol{j}$, $\boldsymbol{j}_{\rm h}$, $j_{\rm s}^{ij} = (j^i\sigma^j + j^j\sigma^i)/2 = [j^i\sigma^j]_{\rm s}$ denote the heat, electric current, thermal current, and spin current, respectively. The odd-parity multipoles are necessary in the lower panel, and the spatial inversion symmetry is broken. The "i" tensors are characterized by the electric (toroidal) multipole, while "c" tensors are characterized by magnetic (toroidal) multipoles. The latter is active only when the time-reversal symmetry is broken.

response	space-time inversion	rank	input	output	relevant multipoles
magneto-carolic coefficient	axial (c)	1	$\boldsymbol{H}$	Q	M_{1m}
Seebeck coefficient	polar (i)	2	$-\boldsymbol{\nabla}T$	$\boldsymbol{E}$	Q_0, G_{1m}, Q_{2m}
spin-current conductivity	axial (i)	3	$\boldsymbol{E}$	$j_{\rm s}^{ij}$	G_{1m}, Q_{2m}, G_{3m}
magneto striction	axial (c)	3	$\boldsymbol{H}$	ε_{ij}	M_{1m}, T_{2m}, M_{3m}
Nernst coefficient	axial (i)	3	$[H^i j_{\rm h}^j]_{\rm s}$	$\boldsymbol{E}$	G_{1m}, Q_{2m}, G_{3m}
electro-carolic coefficient	polar (i)	1	$\boldsymbol{E}$	Q	Q_{1m}
magnetoelectric effect	axial (c)	2	$\boldsymbol{E}$	$\boldsymbol{M}$	M_0, T_{1m}, M_{2m}
Edelstein effect	axial (i)	2	$\boldsymbol{j}$	$\boldsymbol{M}$	G_0, Q_{1m}, G_{2m}
piezoelectric effect	polar (i)	3	ε_{ij}	$\boldsymbol{E}$	Q_{1m}, G_{2m}, Q_{3m}
current-induced strain effect	polar (c)	3	$\boldsymbol{j}$	ε_{ij}	T_{1m}, M_{2m}, T_{3m}

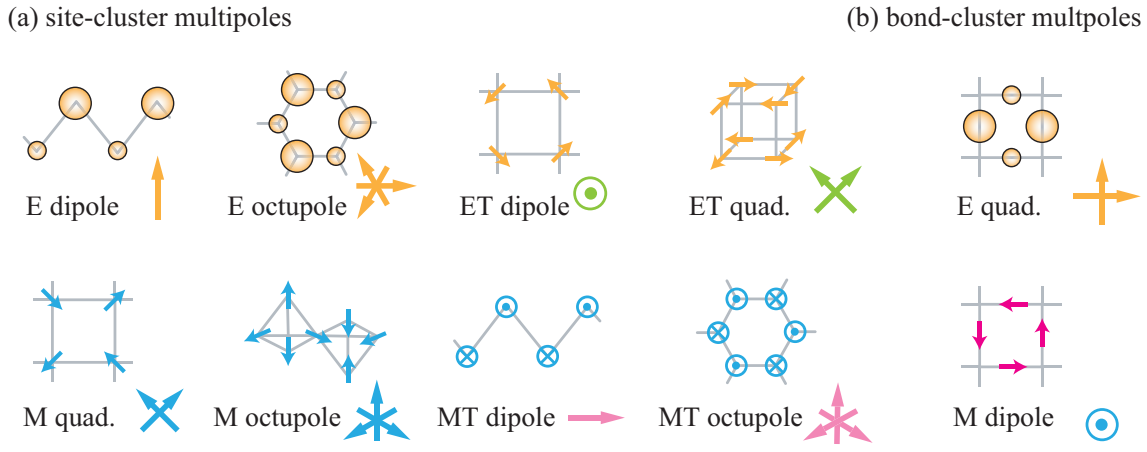

Figure 2. Examples of (a) site-cluster multipoles and (b) bond-cluster multipoles. The correspondences between the alignments of charge or magnetic moment or hopping modulations, and the cluster multipole are shown. The red arrows in the bond-cluster multipoles represent the imaginary hopping modulation.

For example, $\boldsymbol{Q} = 0$ non-collinear magnetic structure found in the hexagonal antiferromagnet Mn_3Sn corresponds to the cluster magnetic octupole or anisotropic magnetic dipole order, and the magnitude of the cluster multipole has a strong correlation with the giant anomalous Hall coefficient despite that the net magnetization is very small [56, 44]. However, following the discussion in the previous section, anomalous Hall conductivity must be related to less than rank 2 multipoles. It is considered that the cluster magnetic octupole, which is a localized degree of freedom, may be related to the Hall conductivity via the Berry curvature (axial vector)

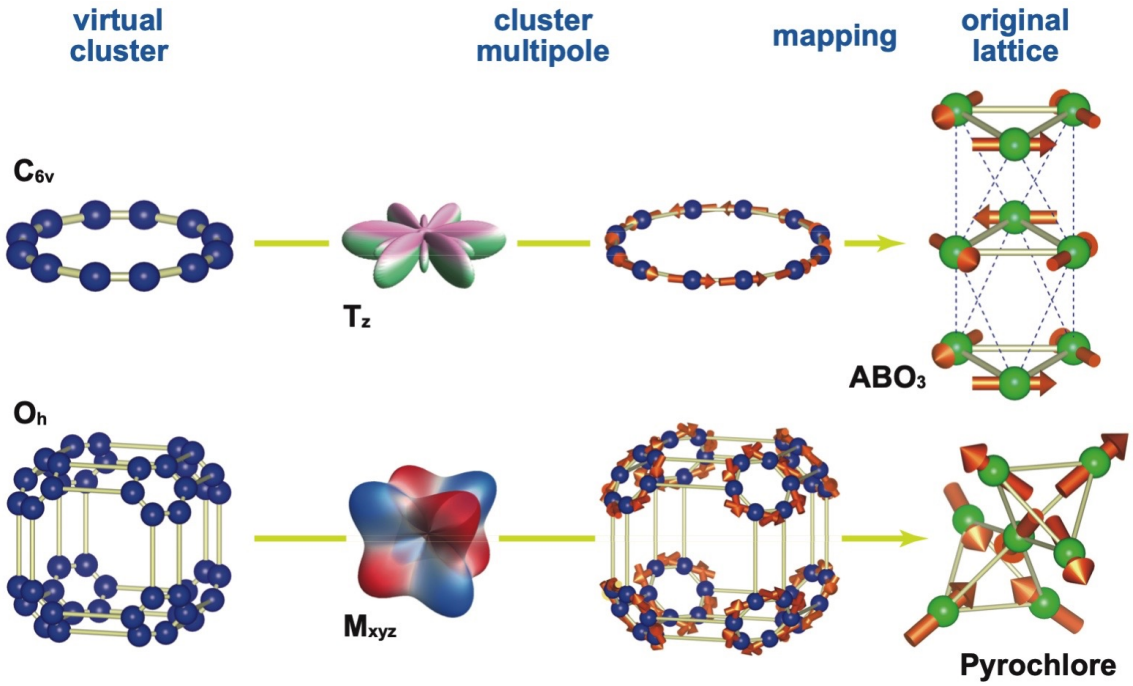

Figure 3. Outline of the generation procedure of the symmetry-adapted magnetic structure basis set. See [71] in detail.

defined in the momentum space [44, 57]. Similarly, $\boldsymbol{Q} = 0$ antiferromagnetic order in the zig-zag structure can be regarded as the cluster magnetic toroidal dipole order [40, 58, 5, 59, 46]. From these viewpoints, one can immediately conclude that the occurrence of the magnetoelectric effect or the non-reciprocal magnon dispersion [59, 60] with no inversion symmetry in such magnetic ordering. With the concept of the site-cluster multipole, the analyses for the current-induced magnetization effect [41, 61, 62] observed in UNi_4B and Ce_3TiBi_5, the magnetic-field-angle controlled electric polarization [63, 64, 65, 48, 66] found in $Co_4Nb_2O_9$, the current-induced strain [31] in $BaMn_2As_2$, the non-reciprocal magnon [67, 68, 69, 59, 70] observed in α-$Cu_2V_2O_7$, etc. are in progress.

One of the important applications of the site-cluster multipole is the generation of the symmetry-adapted magnetic structure basis [71, 72, 73, 74]. To obtain a stable solution especially for non-collinear magnetic structure in the density-functional theory, it is significant to use the symmetry-adapted magnetic structure basis. The outline of the basis generation scheme using the site-cluster multipole is as follows.

First, we set up a virtual cluster consisting of general points of the corresponding point group of the original lattice, where the symmetry operations except the partial translations are common between the original space group and the point group of the virtual cluster. Then, we construct the symmetry-adapted magnetic structures on the virtual cluster corresponding to the site-cluster magnetic or magnetic toroidal multipoles from the lowest rank. By mapping back the obtained magnetic structure basis to the original lattice, the resultant magnetic structures constitute the symmetry-adapted basis set in the original lattice. The outline of the generation procedure is shown in Fig. 3. It should be emphasized that the resultant multipole basis set is uniquely determined irrespective of the choice of the unit cell and the origin of the original lattice.

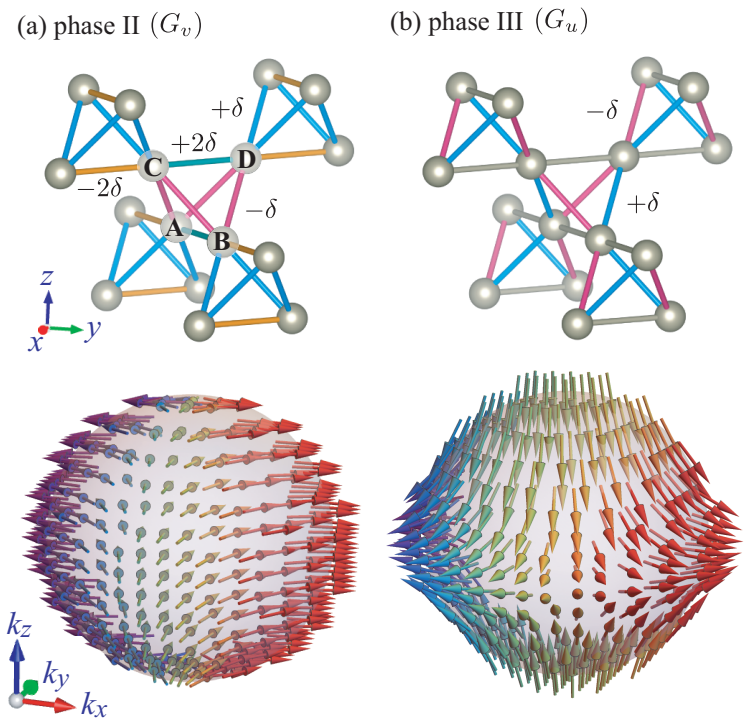

Figure 4. Inversion-symmetry breaking in $Cd_2Re_2O_7$ by the electric toroidal quadrupoles [12].

6. Bond-cluster multipole

The concept of the cluster multipole can also be applied to a modulation of electron hopping. A spontaneous modulation of electron hopping amplitude is usually called the bond ordering. Such a hopping modulation degree of freedom can also be classified according to the point-group symmetry, and it is regarded as a bond-cluster multipole [12, 15]. Considering a one-body tight-binding model, and the site potentials and hopping amplitudes are expressed in a matrix form of the sublattice, the diagonal degrees of freedom are described by the site-cluster multipoles, while the off-diagonal ones are described by the bond-cluster multipoles. Since the hopping amplitude is complex in general, one can consider real and imaginary modulations. By symmetry operations, the real hopping amplitude is transformed like a point charge on the center of the corresponding bond. Similarly, the imaginary hopping amplitude is transformed like a magnetic toroidal dipole along the bond at the center. Therefore, these hopping amplitude degrees of freedom can be expressed by the bond-cluster multipoles, which consist of a specific arrangement of point charges or magnetic toroidal dipoles on the bond centers. See, Fig. 2(b) for example. Note again that in order to construct a unique symmetry-adapted basis set in crystal systems, mapping to the virtual cluster is useful as discussed in the last section.

An example application of the bond-cluster multipole is the spontaneous inversion-symmetry breaking [75, 76, 77, 78, 79, 12] observed in $Cd_2Re_2O_7$. The X-ray diffraction measurements have shown that the symmetry of the system changes from $Fd\bar{3}m$ in the disordered phase (phase I) to $I\bar{4}m2$ in the intermediate phase (phase II) and to $I4_122$ in the low temperature phase (phase III) [75]. The associated point groups are O_h, D_{2d}, and D_4, respectively.

By considering the facts of these experiments, compatibility relation in Table 2, and no magnetic anomaly [80] observed at the phase transitions, the plausible candidate of the order parameters are the electric toroidal quadrupole (ETQ), G_v and G_u in the phases II and III, respectively [12]. Furthermore, the considerably small structural changes indicate that these

transitions are caused by electronic origin [81]. Since the Re d orbitals are dominant components near the Fermi level, the hybrid multipoles might be inactive in this compound. The even-parity atomic multipoles are only active within d orbitals, and the Re ions are located at inversion center. Thus, the ordinary on-site order parameters cannot break the inversion symmetry. By taking these observations into account, the bond ordering is the most plausible candidate of order parameter in this system. The candidate order parameters (hopping amplitude modulations) are depicted in the upper panel of Fig. 4. These order parameters breaking the inversion symmetry cause the spin splitting in the electronic band structure via the spin-orbit coupling. The expected spin splittings are shown in the lower panel of Fig. 4.

In the presence of the ETQs, the current-induced magnetization is expected as discussed in section 4. Moreover, under the external magnetic field, one expects the non-reciprocal current proportional to the square of the external electric fields and current-induced strain. As these 4th rank response tensors contain the information of the ETQ order parameters, the related experiments are on-going. The analysis of the microscopic origin of such bond orderings is left for future study.

7. Band structure in terms of multipole

When an expectation value of a certain multipole becomes finite, it acts as a molecular field yielding a band deformation and/or spin splitting according to its symmetry. Since the Hamiltonian must be fully symmetric with respect to any symmetry operations, one-body hopping-type Hamiltonian (for a single band) is expressed in a "scalar" form [8] as[4]

$$H = \sum_{\boldsymbol{k}} \sum_{\sigma\sigma'} \sum_{lm} X_{lm}^{\sigma\sigma'}(\boldsymbol{k}) X_{lm}^{\mathrm{ext}*} c_{\boldsymbol{k}\sigma}^{\dagger} c_{\boldsymbol{k}\sigma'}, \tag{2}$$

where $c_{\boldsymbol{k}\sigma}^{\dagger}$ ($c_{\boldsymbol{k}\sigma}$) is creation (annihilation) operator of electron with the momentum $\boldsymbol{k}$ and spin σ. Here, X_{lm}^{ext} is the source of molecular field due to the presence of finite expectation value of the multipole X_{lm}. An ordinary form of the tight-binding model is always rearranged in terms of the Fourier transform of the multipole degrees of freedom $X_{lm}(\boldsymbol{k})$ as Eq. (2). When a phase transition characterized by a certain multipole takes place, one can immediately identify which type of band deformation and/or spin splitting occurs from Eq. (2).

For example, since the electric dipole, magnetic toroidal dipole, and electric octupole are expressed as $\boldsymbol{Q}(\boldsymbol{k}) \propto \boldsymbol{k} \times \boldsymbol{\sigma}$, $\boldsymbol{T}(\boldsymbol{k}) \propto \boldsymbol{k}$, $Q_{xyz}(\boldsymbol{k}) \propto k_x(k_y^2 - k_z^2)\sigma_x + k_y(k_z^2 - k_x^2)\sigma_y + k_z(k_x^2 - k_y^2)\sigma_z$ in the momentum space, the polar (molecular) electric field $\boldsymbol{Q}^{\mathrm{ext}}$ causes the Rashba spin splitting via the anti-symmetric spin-orbit coupling, $\boldsymbol{Q}(\boldsymbol{k}) \cdot \boldsymbol{Q}^{\mathrm{ext}}$. Similarly, in the cubic systems without inversion symmetry, e.g., T_{d}, Q_{xyz}^{ext} can exist as it belongs to the identity irreducible representation. In this case, the Dresselhaus spin-orbit coupling, $Q_{xyz}(\boldsymbol{k})Q_{xyz}^{\mathrm{ext}}$ causes rather complicated spin splitting. Moreover, in the presence of $\boldsymbol{T}^{\mathrm{ext}}$, the band shift with keeping spin degeneracy occurs through the coupling $\boldsymbol{T}(\boldsymbol{k}) \cdot \boldsymbol{T}^{\mathrm{ext}}$. In this way, the band deformations in the presence of the multipole ordering are easily identified by means of Eq. (2). Examples of typical band deformations are shown in Fig. 5. The spin splitting occurs only when the product of time-reversal $\mathcal{T}$ and inversion $\mathcal{P}$ symmetries is broken. On the other hand, the anti-symmetric band deformation with spin degeneracy requires both $\mathcal{T}$ and $\mathcal{P}$ breakings with preserving $\mathcal{TP}$. The relation between the band deformations and the source multipoles is summarized[5] in Table. 4.

---

[4] For simplicity, we consider the situation as $\boldsymbol{k} \sim 0$. For general $\boldsymbol{k}$, the periodicity of the lattice must be considered, e.g., $k_x \to \sin(k_x a)$, $k_x^2 \to \cos(k_x a)$ and so on.

[5] Note that in the case of single-band system, the operator expressions of the odd-parity $M_{lm}(\boldsymbol{k})$ (l =even) and even-parity $G_{lm}(\boldsymbol{k})$ (l =odd) do not exist. For these multipoles, an effective spin-orbital entanglement band structure denoted as "spin-orbital-momentum locking occurs in the multi-orbital system [82].

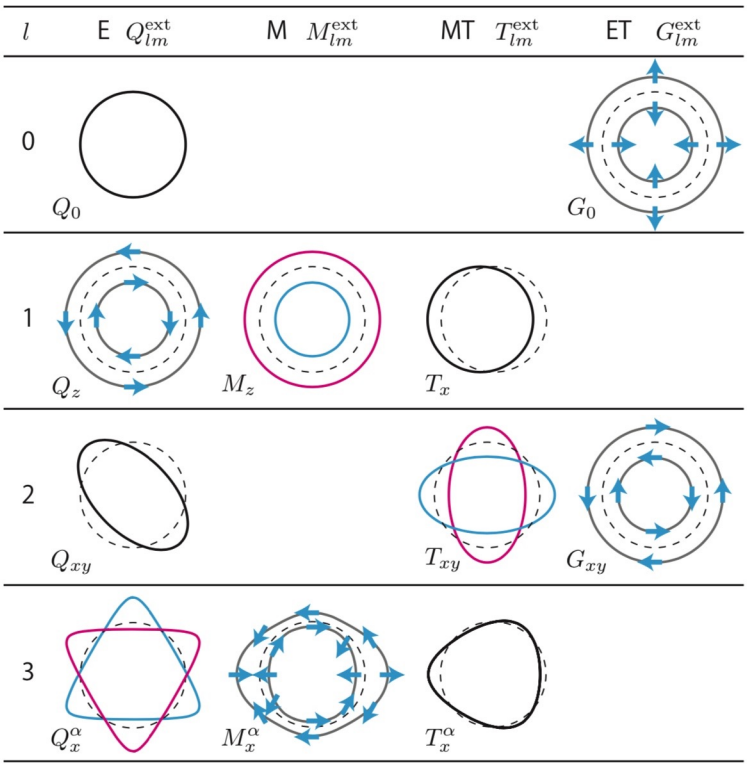

Figure 5. Examples of band-structure deformation ($k_z = 0$ plane) due to the presence of multipoles [8]. The dashed line represents the band structure due to the pure electric monopole, $Q_0 \propto k_x^2 + k_y^2$. The red (blue) line represents the up (down) spin component, while the arrows represent the in-plane components.

Table 4. Band modulation and corresponding multipoles [8]。

type of deformation	l =even	l =odd
symmetric modulation	$Q_{lm}^{\rm ext}$	$G_{lm}^{\rm ext}$
anti-symmetric modulation	$M_{lm}^{\rm ext}$	$T_{lm}^{\rm ext}$
symmetric spin splitting	$T_{lm}^{\rm ext}$	$M_{lm}^{\rm ext}$
anti-symmetric spin splitting	$G_{lm}^{\rm ext}$	$Q_{lm}^{\rm ext}$

From this perspective, it is possible to generate a spin-orbit-like coupling by the antiferromagnetic orderings without the atomic spin-orbit coupling. For example, it is often understood that a spin splitting originates from the atomic spin-orbit coupling, however, it can arise when the multipoles listed in the lower panel of Table. 4 become active [13, 14, 15]. As an example, we show the case of the collinear $\boldsymbol{Q} = 0$ antiferromagnetic ordering in the sublattice system [13]. The $\boldsymbol{k}$ component of the molecular-field Hamiltonian of such a system is described in the following form,

$$H(\boldsymbol{k}) = \sum_{\Gamma\gamma} Q_{\Gamma\gamma}^{\text{bond-cluster}} Q_{\Gamma\gamma}(\boldsymbol{k}) - \sum_{\Gamma\gamma} Q_{\Gamma\gamma}^{\text{site-cluster}} h_{\Gamma\gamma}\sigma, \tag{3}$$

where the first term is the hopping term, and the second term is the molecular field due to $\boldsymbol{Q} = 0$ collinear antiferromagnetic order in the sublattice, and Γ and γ are the irreducible representation and its component. Let us consider a certain alignment of antiferromagnetic ordering that occurs in the sublattice, e.g., $\gamma = xy$-type. The molecular field, h_{xy}, induces quantities belonging to the same irreducible representation and component as $h_{xy}\sigma \to Q_{xy}^{\text{site-cluster}} \to Q_{xy}^{\text{bond-cluster}} \to Q_{xy}(\boldsymbol{k})$. As a result, the effective coupling as $Q_{xy}(\boldsymbol{k})\sigma$ arises. Since $Q_{xy}(\boldsymbol{k}) \sim k_x k_y$, we obtain xy-type spin splitting. Note that within the collinear magnetic ordering in the absence of the spin-orbit coupling, we obtain only the symmetric spin splitting which is proven by using the spin rotation. A spin-current generation by means of this symmetric spin-splitting is proposed in the organic conductor and the $3d$ transition metal oxide with relatively weak spin-orbit coupling [83, 84, 85, 86].

In the case of the non-collinear magnetic ordering, e.g., 120° structure in the trigonal lattices, the anti-symmetric spin splitting is also expected [14, 15]. The higher-order coupling between the antiferromagnetic order parameter and the multipole in the momentum space is the origin of the anti-symmetric spin splitting. Moreover, in a way similar to decomposing the tight-binding Hamiltonian, the spin exchange coupling can also be decomposed by the multipole basis set. Then, the possibility of generating effective Dzyaloshinskii-Moriya interaction without spin-orbit coupling is examined [87].

8. Summary

In this paper, we have shown that the concept of multipole is extremely useful and allows us to deal with physical phenomena in a general and comprehensive manner. Using the symmetry-adapted multipole basis set, which consists of the site-cluster or bond-cluster basis with atomic multipole on each cluster site, not only electronic degrees of freedom, but also the lattice deformation (phonon dispersion), two-body interaction including spin exchange coupling and so on are also expressed and classified according to the crystallographic point group. Such a description provides a new direction in the fields of materials design and informatics where the symmetry-adapted multipole can be used as a good descriptor or a building block of the neural network.

This paper is based on fruitful collaborations with Yuki Yanagi, Megumi Yatsushiro, Rikuto Oiwa, Makoto Naka, Michi-to Suzuki, Yukitoshi Motome, Hitoshi Seo, Takuya Nomoto, and Ryotaro Arita. We would also like to thank Hiroshi Amitsuka, Hisatomo Harima, Yoichi Yanase, Takahisa Arima, Zenji Hiroi, Hiraku Saito, Akira Oyamada, and many others for helpful discussions. This work was supported by Grant-in-Aid for Scientific Research Nos. JP15H05885, JP18H04296 (J-Physics), JP18K13488, JP19K03752, JP19H01834, JP21H01031, and JP21H01037.

[1] H. Kusunose: J. Phys. Soc. Jpn. **77** (2008) 064710.
[2] Y. Kuramoto, H. Kusunose, and A. Kiss: J. Phys. Soc. Jpn. **78** (2009) 072001.
[3] P. Santini, S. Carretta, G. Amoretti, R. Caciuffo, N. Magnani, and G. H. Lander: Rev. Mod. Phys. **81** (2009) 807.
[4] M.-T. Suzuki, H. Ikeda, and P. M. Oppeneer: J. Phys. Soc. Jpn. **87** (2018) 041008.
[5] S. Hayami, H. Kusunose, and Y. Motome: J. Phys.: Condens. Matter **28** (2016) 395601.
[6] M. Matsumoto, K. Chimata, and M. Koga: J. Phys. Soc. Jpn. **86** (2017) 034704.
[7] S. Hayami and H. Kusunose: J. Phys. Soc. Jpn. **87** (2018) 033709.
[8] S. Hayami, M. Yatsushiro, Y. Yanagi, and H. Kusunose: Phys. Rev. B **98** (2018) 165110.
[9] H. Watanabe and Y. Yanase: Phys. Rev. B **98** (2018) 245129.
[10] S. Sumita and Y. Yanase: Phys. Rev. Research **2** (2020) 033225.
[11] H. Kusunose, R. Oiwa, and S. Hayami: J. Phys. Soc. Jpn. **89** (2020) 104704.
[12] S. Hayami, Y. Yanagi, H. Kusunose, and Y. Motome: Phys. Rev. Lett. **122** (2019) 147602.
[13] S. Hayami, Y. Yanagi, and H. Kusunose: J. Phys. Soc. Jpn. **88** (2019) 123702.
[14] S. Hayami, Y. Yanagi, and H. Kusunose: Phys. Rev. B **101** (2020) 220403(R).

[15] S. Hayami, Y. Yanagi, and H. Kusunose: Phys. Rev. B **102** (2020) 144441.
[16] M. Yatsushiro, H. Kusunose, and S. Hayami: Phys. Rev. B **104** (2021) 054412.
[17] R. Oiwa and H. Kusunose: J. Phys. Soc. Jpn. **91** (2022) 014701.
[18] C. Schwartz: Phys. Rev. **97** (1955) 380.
[19] J. M. Blatt and V. F. Weisskopf: *Theoretical Nuclear Physics* (Dover Publications, New York, 1991).
[20] J. D. Jackson: *Classical Electrodynamics, Third Edition* (John Wiley and Sons, Inc., 1 1999).
[21] V. Dubovik and A. Cheshkov: Sov. J. Part. Nucl **5** (1975) 318.
[22] V. Dubovik, L. Tosunyan, and V. Tugushev: Zh. Eksp. Teor. Fiz **90** (1986) 590.
[23] V. Dubovik and V. Tugushev: Phys. Rep. **187** (1990) 145.
[24] A. Gorbatsevich and Y. V. Kopaev: Ferroelectrics **161** (1994) 321.
[25] N. A. Spaldin, M. Fiebig, and M. Mostovoy: J. Phys.: Condens. Matter **20** (2008) 434203.
[26] Y. V. Kopaev: Physics-Uspekhi **52** (2009) 1111.
[27] J. Hlinka: Phys. Rev. Lett. **113** (2014) 165502.
[28] S. Nanz: *Toroidal Multipole Moments in Classical Electrodynamics: An Analysis of Their Emergence and Physical Significance* (Springer, 2016).
[29] T. Furukawa, Y. Shimokawa, K. Kobayashi, and T. Itou: Nat. Commun. **8** (2017) 954.
[30] T. Yoda, T. Yokoyama, and S. Murakami: Nano letters **18** (2018) 916.
[31] H. Watanabe and Y. Yanase: Phys. Rev. B **96** (2017) 064432.
[32] S. Tsubouchi, T. Kyômen, M. Itoh, P. Ganguly, M. Oguni, Y. Shimojo, Y. Morii, and Y. Ishii: Phys. Rev. B **66** (2002) 052418.
[33] J. Kuneš and P. Augustinský: Phys. Rev. B **90** (2014) 235112.
[34] T. Kaneko and Y. Ohta: Phys. Rev. B **94** (2016) 125127.
[35] T. Yamaguchi, K. Sugimoto, and Y. Ohta: Physica B: Condensed Matter (2017).
[36] R. Hanson, L. P. Kouwenhoven, J. R. Petta, S. Tarucha, and L. M. K. Vandersypen: Rev. Mod. Phys. **79** (2007) 1217.
[37] C. H. Greene, P. Giannakeas, and J. Pérez-Ríos: Rev. Mod. Phys. **89** (2017) 035006.
[38] S. Watanabe and K. Miyake: J. Phys. Soc. Jpn. **88** (2019) 033701.
[39] T. Arima: J. Phys. Soc. Jpn. **82** (2013) 013705.
[40] Y. Yanase: J. Phys. Soc. Jpn. **83** (2014) 014703.
[41] S. Hayami, H. Kusunose, and Y. Motome: Phys. Rev. B **90** (2014) 024432.
[42] S. Hayami, H. Kusunose, and Y. Motome: Phys. Rev. B **90** (2014) 081115.
[43] T. Hitomi and Y. Yanase: J. Phys. Soc. Jpn. **83** (2014) 114704.
[44] M.-T. Suzuki, T. Koretsune, M. Ochi, and R. Arita: Phys. Rev. B **95** (2017) 094406.
[45] T. Hitomi and Y. Yanase: J. Phys. Soc. Jpn. **85** (2016) 124702.
[46] S. Sumita and Y. Yanase: Phys. Rev. B **93** (2016) 224507.
[47] Y. Yanagi and H. Kusunose: J. Phys. Soc. Jpn. **86** (2017) 083703.
[48] Y. Yanagi, S. Hayami, and H. Kusunose: Phys. Rev. B **97** (2018) 020404.
[49] S. Hayami, H. Kusunose, and Y. Motome: Phys. Rev. B **97** (2018) 024414.
[50] T. Ishitobi and K. Hattori: J. Phys. Soc. Jpn. **88** (2019) 063708.
[51] S. Hayami, H. Kusunose, and Y. Motome: J. Phys. Soc. Jpn. **88** (2019) 063702.
[52] M. Yatsushiro and S. Hayami: J. Phys. Soc. Jpn. **89** (2020) 013703.
[53] M. Yatsushiro and S. Hayami: Phys. Rev. B **102** (2020) 195147.
[54] T. Nomoto and R. Arita: Phys. Rev. Research **2** (2020) 012045.
[55] M. Yatsushiro, R. Oiwa, H. Kusunose, and S. Hayami: Phys. Rev. B **105** (2022) 155157.
[56] S. Nakatsuji, N. Kiyohara, and T. Higo: Nature **527** (2015) 212.
[57] S. Hayami and H. Kusunose: Phys. Rev. B **103** (2021) L180407.
[58] S. Hayami, H. Kusunose, and Y. Motome: J. Phys. Soc. Jpn. **84** (2015) 064717.
[59] S. Hayami, H. Kusunose, and Y. Motome: J. Phys. Soc. Jpn. **85** (2016) 053705.
[60] T. Matsumoto and S. Hayami: Phys. Rev. B **104** (2021) 134420.
[61] H. Saito, K. Uenishi, N. Miura, C. Tabata, H. Hidaka, T. Yanagisawa, and H. Amitsuka: J. Phys. Soc. Jpn. **87** (2018) 033702.
[62] M. Shinozaki, G. Motoyama, M. Tsubouchi, M. Sezaki, J. Gouchi, S. Nishigori, T. Mutou, A. Yamaguchi, K. Fujiwara, M. Kiyotaka, and Y. Uwatoko: J. Phys. Soc. Jpn. **89** (2020) 033703.
[63] N. D. Khanh, N. Abe, H. Sagayama, A. Nakao, T. Hanashima, R. Kiyanagi, Y. Tokunaga, and T. Arima: Phys. Rev. B **93** (2016) 075117.
[64] N. D. Khanh, N. Abe, S. Kimura, Y. Tokunaga, and T. Arima: Phys. Rev. B **96** (2017) 094434.
[65] Y. Yanagi, S. Hayami, and H. Kusunose: Physica B: Condensed Matter **536** (2018) 649.
[66] M. Matsumoto and M. Koga: J. Phys. Soc. Jpn. **88** (2019) 094704.

[67] G. Gitgeatpong, Y. Zhao, M. Avdeev, R. O. Piltz, T. J. Sato, and K. Matan: Phys. Rev. B **92** (2015) 024423.
[68] G. Gitgeatpong, M. Suewattana, S. Zhang, A. Miyake, M. Tokunaga, P. Chanlert, N. Kurita, H. Tanaka, T. J. Sato, Y. Zhao, and K. Matan: Phys. Rev. B **95** (2017) 245119.
[69] G. Gitgeatpong, Y. Zhao, P. Piyawongwatthana, Y. Qiu, L. W. Harriger, N. P. Butch, T. J. Sato, and K. Matan: Phys. Rev. Lett. **119** (2017) 047201.
[70] R. Takashima, Y. Shiomi, and Y. Motome: Phys. Rev. B **98** (2018) 020401.
[71] M.-T. Suzuki, T. Nomoto, R. Arita, Y. Yanagi, S. Hayami, and H. Kusunose: Phys. Rev. B **99** (2019) 174407.
[72] V. T. N. Huyen, M.-T. Suzuki, K. Yamauchi, and T. Oguchi: Phys. Rev. B **100** (2019) 094426.
[73] M.-T. Huebsch, T. Nomoto, M. T. Suzuki, and R. Arita: Phys. Rev. X **11** (2021) 011031.
[74] Y. Yanagi, H. Kusunose, T. Nomoto, R. Arita, and M.-T. Suzuki: arXiv:2201.07361 (2022).
[75] J.-I. Yamaura and Z. Hiroi: J. Phys. Soc. Jpn. **71** (2002) 2598.
[76] I. A. Sergienko and S. H. Curnoe: J. Phys. Soc. Jpn. **72** (2003) 1607.
[77] T. C. Kobayashi, Y. Irie, J.-i. Yamaura, Z. Hiroi, and K. Murata: J. Phys. Soc. Jpn. **80** (2011) 023715.
[78] J.-i. Yamaura, K. Takeda, Y. Ikeda, N. Hirao, Y. Ohishi, T. C. Kobayashi, and Z. Hiroi: Phys. Rev. B **95** (2017) 020102.
[79] Z. Hiroi, J.-i. Yamaura, T. C. Kobayashi, Y. Matsubayashi, and D. Hirai: J. Phys. Soc. Jpn. **87** (2017) 024702.
[80] O. Vyaselev, K. Arai, K. Kobayashi, J. Yamazaki, K. Kodama, M. Takigawa, M. Hanawa, and Z. Hiroi: Phys. Rev. Lett. **89** (2002) 017001.
[81] J. P. Castellan, B. D. Gaulin, J. van Duijn, M. J. Lewis, M. D. Lumsden, R. Jin, J. He, S. E. Nagler, and D. Mandrus: Phys. Rev. B **66** (2002) 134528.
[82] S. Hayami and H. Kusunose: Phys. Rev. B **104** (2021) 045117.
[83] M. Naka, S. Hayami, H. Kusunose, Y. Yanagi, Y. Motome, and H. Seo: Nature communications **10** (2019) 4305.
[84] S. Hayami, Y. Yanagi, M. Naka, H. Seo, Y. Motome, and H. Kusunose: JPS Conf. Proc. **30** (2020) 011149.
[85] M. Naka, Y. Motome, and H. Seo: Phys. Rev. B **103** (2021) 125114.
[86] S. Hayami and M. Yatsushiro: J. Phys. Soc. Jpn. **91** (2022) 063702.
[87] T. Matsumoto and S. Hayami: Phys. Rev. B **101** (2020) 224419.